The College of Engineering
University of Wisconsin-Madison

Wisconsin Electric Machines and Power Electronics Consortium

RESEARCH REPORT
93-40

Current Sensorless Field Oriented Control of Synchronous Reluctance Motor

Takayoshi Matsuo, Thomas A. Lipo
Dept. of Electrical and Computer Engineering
University of Wisconsin-Madison
1415 Johnson Drive
Madison, WI 53706

WEMPEC

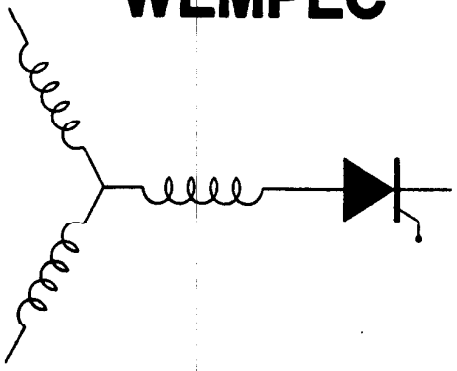

Department of Electrical and Computer Engineering
1415 Johnson Drive
Madison, Wisconsin 53706

Current Sensorless Field Oriented Control of Synchronous Reluctance Motor

Takayoshi Matsuo and Thomas A. Lipo
University of Wisconsin-Madison
Electrical and Computer Engineering
1415 Johnson Drive
Madison, Wisconsin 53706

***Abstract*– It is the purpose of this paper to propose and examine a control strategy for a synchronous reluctance motor which eliminates the need for having a current sensor. In this work, control strategies, practical implementation and performance of a current sensorless field oriented control for a synchronous reluctance motor is presented. A field oriented control scheme without current sensors which includes the voltage reference calculator which generates the required voltage references from the torque command and the motor speed is proposed. Excellent control performance has been obtained, which indicates that current sensorless field oriented control of synchronous reluctance motors can be applicable in practical high performance drive systems.**

INTRODUCTION

The synchronous reluctance motor has recently attracted the efforts of a number of researchers [1-5] and is gaining increasing interest as a possible alternative for ac drives. The synchronous reluctance motor is a singly salient machine in which the rotor is constructed so as to employ the principle of reluctance torque to produce electromechanical energy conversion. Only the rotor is constructed with salient poles while the stator inner surface is cylindrical and typically wound in an identical manner to an induction machine. A configuration for a modern axially laminated four pole machine is illustrated in Fig. 1 [5]. Specifically, the rotor is assumed to be constructed of "packets" of thin laminations which are bent in a semi-circular shape. These thick packets of steel are assumed to separated by a suitable insulator, perhaps air, but also possibly, plastic laminate or epoxy-like material. All of the lamination segments are assumed to be equally spaced. It has been demonstrated that there exists an optimized rotor design for a synchronous reluctance motor, which is based on the optimization of two important factors, i.e., the "motor torque index", (L_{ds}-L_{qs}) and the saliency ratio, L_{ds}/L_{qs}. It has been shown that the motor power factor of 0.8 is a realizable value while the "motor torque index", (L_{ds}-L_{qs}) is maintained at maximum level with the optimized rotor design. The machine typically retains many of the benefits of variable reluctance motors while at the same time eliminating several of its disadvantages. The noise and torque pulsation problems, so difficult to overcome with variable reluctance motors, can be elegantly overcome in a synchronous reluctance machine by simply winding the stator in the conventional manner so as to produce a sinusoidal uniformly rotating air gap MMF. A field oriented control scheme with the decoupled current controller, the variable d-q current limit and the variable speed loop gain for synchronous reluctance motors has already been proposed [4] and resulting the excellent control performance has indicated that the synchronous reluctance motors can be suitably applied to high performance drive systems.

It is the purpose of this paper to propose and examine another control strategy for synchronous reluctance motors which eliminates the need for having a current sensor.

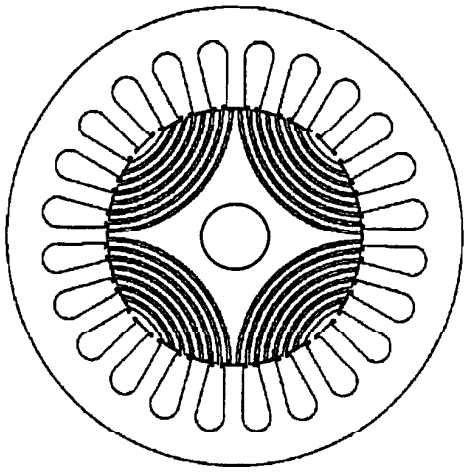

Fig. 1 A configuration of a synchronous reluctance motor.

d-q EQUATIONS FOR THE SYNCHRONOUS RELUCTANCE MOTOR

The equations which describe the behavior of the synchronous reluctance motor can be derived from the conventional equations depicting a conventional wound field

synchronous machine, that is Park's Equations. In such machines, the excitation (field) winding is non-existent. Also, in machines typically employing a modern axially laminated rotor structure, a rotor cage is normally omitted since the machine can be started synchronously from rest by proper inverted control. Hence, eliminating both the field winding and damper winding equations from Park's equations forms the basis for the d-q Equations for a synchronous reluctance machine. That is,

$$v_{ds} = r_s i_{ds} + \frac{d}{dt}\lambda_{ds} - \omega_r \lambda_{qs} \quad (1)$$

$$v_{qs} = r_s i_{qs} + \frac{d}{dt}\lambda_{qs} + \omega_r \lambda_{ds} \quad (2)$$

$$\lambda_{ds} = L_{ls} i_{ds} + L_{md} i_{ds} \quad (3)$$

$$\lambda_{qs} = L_{ls} i_{qs} + L_{mq} i_{qs} \quad (4)$$

where L_{md}, L_{mq} and L_{ls} are, respectively, the direct axis and quadrature axis magnetizing inductances and the stator leakage inductance. The quantity r_s is the stator resistance per phase and ω_r is the angular speed of the rotor in equivalent electrical radians per second. In terms of the d-q variables, the electromagnetic torque is described as

$$T_e = \frac{3}{2}\frac{P}{2}(L_{ds} - L_{qs}) i_{ds} i_{qs} \quad (5)$$

where P is the number of poles.

PHASOR EQUATIONS FOR A SYNCHRONOUS RELUCTANCE MOTOR

A single phasor equation can be derived from the steady state version of Eqs. 1 and 2 by setting the d/dt terms to zero and then multiplying Eqs. 1 by $-j$ and adding it to Eq. 2. The result is

$$V_{qs} - jV_{ds} = r_s(I_{qs} - jI_{ds}) + \omega_e(\lambda_{ds} + j\lambda_{qs}) \quad (6)$$

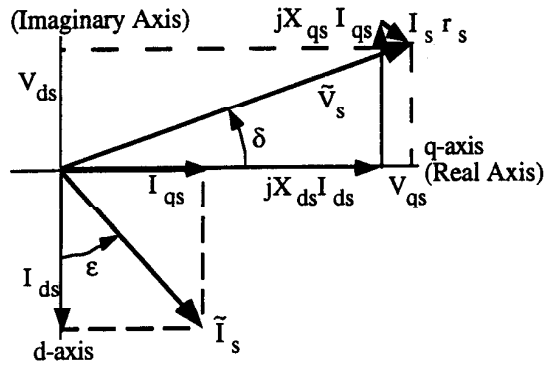

Fig. 2 Phasor diagram for synchronous reluctance machine.

or, using Eqs. 3 and 4,

$$V_{qs} - jV_{ds} = r_s(I_{qs} - jI_{ds}) + \omega_e(L_{ds}I_{ds} + jL_{qs}I_{qs}) \quad (7)$$

Equation 7 can be manipulated to form

$$V_{qs} - jV_{ds} = r_s(I_{qs} - jI_{ds}) + j\omega_e(-jL_{ds}I_{ds} + L_{qs}I_{qs}) \quad (8)$$

or

$$V_{qs} - jV_{ds} = r_s(I_{qs} - jI_{ds}) + j\omega_e L_{ds}(-jI_{ds}) + j\omega_e L_{qs} I_{qs} \quad (9)$$

In phasor notation

$$\tilde{V}_s = r_s \tilde{I}_s + jX_{ds}\tilde{I}_{ds} + jX_{qs}\tilde{I}_{qs} \quad (10)$$

A phasor diagram of Equation 10 is shown in Fig. 2.

FIELD ORIENTED CONTROL OF SYNCHRONOUS RELUCTANCE MOTOR

The torque of a synchronous reluctance machine can be controlled by controlling the d- and q-axis current, i_{ds} and i_{qs}, independently. Consider first, the current versus load profile. It can be recalled that in the case of an induction motor, the rotor flux is held constant while component of stator current flowing in the rotor resistor R_2/S is varied with the torque demand. In general, this is done due to the fact that the rotor flux producing component of stator current affects the torque very slowly due to the long rotor time constant. However, in the case of the synchronous reluctance machine, no rotor windings exist to oppose this flux producing component. Hence, the rotor flux can be changed much more rapidly so that both the flux and torque producing components can be increased as desired to satisfy the torque and another criterion as well. In most cases the conductor losses of the machine will dominate in which case it would be desirable to minimize the conductor I^2R loss. The maximum torque per ampere is obtained by setting MMF angle $\varepsilon = 45°$ in which case $i_{ds} = i_{qs}$. However, this strategy cannot be maintained as load continues to increase since at some point the flux established in the d-axis by i_{ds} begins to exceed the rated flux. Hence, at the point

$$i_{ds} X_{ds} = \omega_e \lambda_{rated} \quad (11)$$

the current i_{ds} must be maintained as constant while the q-axis component i_{qs} continues to increase to satisfy the load. The current i_{qs} continues to increase until rated load is reached (maximum power factor condition). Figure 3 shows the stator current versus load profile.

The maximum power factor operation point is clearly an ideal operating condition for which to define rated torque. It is useful to consider how close is this operating point to the maximum torque condition at pull out. If the stator resistance is neglected, the input power and output power can be equated. The input power for the maximum power factor

condition [6] is, for the case where the stator resistance is neglected

$$P_{pf(max)} = \frac{3}{2} V_s I_s \cos\phi = \frac{3}{2} V_s I_s \frac{L_{ds} - L_{qs}}{L_{ds} + L_{qs}} \quad (12)$$

and

$$V_{qs} = V_s \cos\delta = X_{ds} I_{ds} = X_{ds} I_s \cos\varepsilon \quad (13)$$

$$V_{ds} = V_s \sin\delta = X_{qs} I_{qs} = X_{qs} I_s \sin\varepsilon \quad (14)$$

Taking the ratio of these two equations,

$$\tan\delta = \frac{X_{qs}}{X_{ds}} \tan\varepsilon = \frac{L_{qs}}{L_{ds}} \tan\varepsilon \quad (15)$$

However, from the maximum power factor condition, $\tan\varepsilon = \sqrt{\frac{L_{ds}}{L_{qs}}}$, so that the tangent of the torque angle δ at maximum power factor is

$$\tan\delta = \sqrt{\frac{L_{qs}}{L_{ds}}} \quad (16)$$

From Eqs. 15 and 16 we can easily establish that

$$\cos\varepsilon = \sqrt{\frac{L_{qs}}{L_{ds} + L_{qs}}} \quad (17)$$

$$\cos\delta = \sqrt{\frac{L_{ds}}{L_{ds} + L_{qs}}} \quad (18)$$

Finally, from Eq. 13 the current amplitude at the maximum power factor condition is

$$I_s = \frac{V_s}{X_{ds}} \sqrt{\frac{L_{ds}}{L_{qs}}} \quad (19)$$

Combining Eqs. 12 and 19, the input power now expressed solely in terms of the input voltage as

$$P_{pf(max)} = \frac{3}{2} \frac{V_s^2}{\omega_e} \frac{1}{\sqrt{L_{ds} L_{qs}}} \frac{L_{ds} - L_{qs}}{L_{ds} + L_{qs}} \quad (20)$$

At pullout, the output torque is

$$T_{e(po)} = \frac{3}{4} \frac{P}{2} \left[\frac{1}{L_{qs}} - \frac{1}{L_{ds}}\right] \left(\frac{V_s}{\omega_e}\right)^2 \quad (21)$$

Neglecting losses the input power is

$$P_{po} = \frac{\omega_e}{(P/2)} T_{e(po)}$$

$$= \frac{3}{4} \left[\frac{1}{L_{qs}} - \frac{1}{L_{ds}}\right] \frac{V_s^2}{\omega_e} \quad (22)$$

Taking the ratio of Eq. 22 to 20 results in

$$\frac{P_{po}}{P_{pf(max)}} = \frac{\frac{3}{4} \left[\frac{1}{L_{qs}} - \frac{1}{L_{ds}}\right] \left(\frac{V_s^2}{\omega_e}\right)}{\frac{3}{2} \frac{V_s^2}{\omega_e} \frac{1}{\sqrt{L_{ds} L_{qs}}} \frac{L_{ds} - L_{qs}}{L_{ds} + L_{qs}}} \quad (23)$$

which ultimately reduces to

$$\frac{P_{po}}{P_{pf(max)}} = \frac{1}{2} \frac{L_{ds} + L_{qs}}{\sqrt{L_{ds} L_{qs}}} \quad (24)$$

Hence, if $L_{ds}/L_{qs} = 8.0$, then $P_{po}/P_{pf(max)} = 1.59$ which is a quite reasonable value of per unit pull out torque.

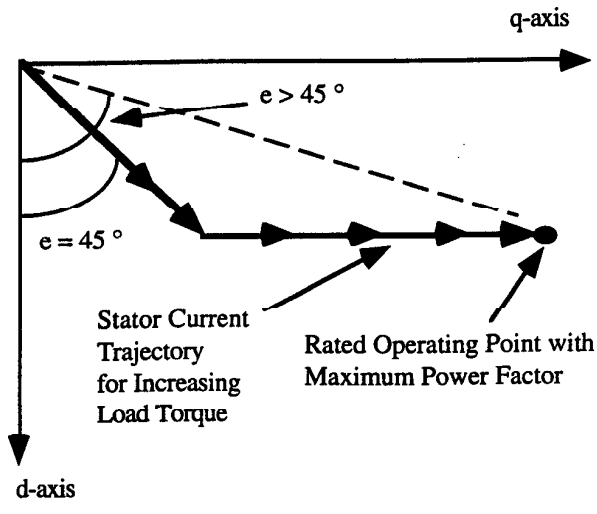

Fig. 3 Locus of the stator current vector as a function of load.

VOLTAGE REFERENCE CALCULATION FOR CURRENT SENSORLESS FIELD ORIENTED CONTROL OF SYNCHRONOUS RELUCTANCE MOTOR

The required d- and q- axis voltage to produce a specified motor torque at a specified motor speed can be obtained from the equations 1-5 and the relationship between the d- and q-axis current which is illustrated in Fig. 3. First, for the region where MMF angle $\varepsilon = 45°$ in which case $i_{ds} = i_{qs}$, the d- and q-axis current, i_{ds} and i_{qs}, are expressed in terms of the motor torque T_e.

$$i_{ds} = \sqrt{\frac{T_e}{\frac{3}{2} \frac{P}{2} (L_{ds} - L_{qs})}} \quad (25)$$

$$i_{qs} = \pm \sqrt{\frac{T_e}{\frac{3}{2}\frac{P}{2}(L_{ds} - L_{qs})}} \quad (26)$$

by inserting Eqs. 25 and 26 into Eqs. 1 and 2, the required voltages v_{ds} and v_{qs} are

$$v_{ds} = \sqrt{\frac{1}{\frac{3}{2}\frac{P}{2}(L_{ds} - L_{qs})}} * \left(r_s \sqrt{T_e} + L_{ds} \frac{d\sqrt{T_e}}{dt} \mp L_{qs}\, \omega_r \sqrt{T_e} \right) , \quad (27)$$

$$v_{qs} = \sqrt{\frac{1}{\frac{3}{2}\frac{P}{2}(L_{ds} - L_{qs})}} * \left(\pm r_s \sqrt{T_e} + L_{qs} \frac{\pm d\sqrt{T_e}}{dt} + L_{ds}\, \omega_r \sqrt{T_e} \right) \quad (28)$$

where + sign is used for $T_e>0$ and - sign for $T_e<0$ in Eqs. 26-28.

Next, for the region where d-axis current i_{ds} is kept constant at i_{dsmax}, the q-axis current expressed in terms of T_e and i_{dsmax} is

$$i_{qs} = \frac{1}{\frac{3}{2}\frac{P}{2}(L_{ds} - L_{qs})\, i_{dsmax}} T_e \quad (29)$$

By inserting Eq. 29 into Eqs. 1 and 2, the required voltages v_{ds} and v_{qs} are

$$v_{ds} = r_s\, i_{dsmax} - \frac{L_{qs}}{\frac{3}{2}\frac{P}{2}(L_{ds} - L_{qs})\, i_{dsmax}} \omega_r T_e \quad (30)$$

$$v_{qs} = \frac{1}{\frac{3}{2}\frac{P}{2}(L_{ds} - L_{qs})\, i_{dsmax}} \left(r_s T_e + L_{qs} \frac{dT_e}{dt} \right) + \omega_r L_{ds}\, i_{dsmax} \quad (31)$$

For the region where the absolute value of the motor torque is less than $T_{e@idmax}$, the required voltages are given by the Eqs. 27 and 28, and for the region where the absolute value of the motor torque is greater than $T_{e\text{-}idmax}$, the required voltages are given by the Eqs. 30 and 31, where

$$T_{e@idmax} = \frac{3}{2}\frac{P}{2}(L_{ds} - L_{qs})\, i_{dsmax}^2 \quad (32)$$

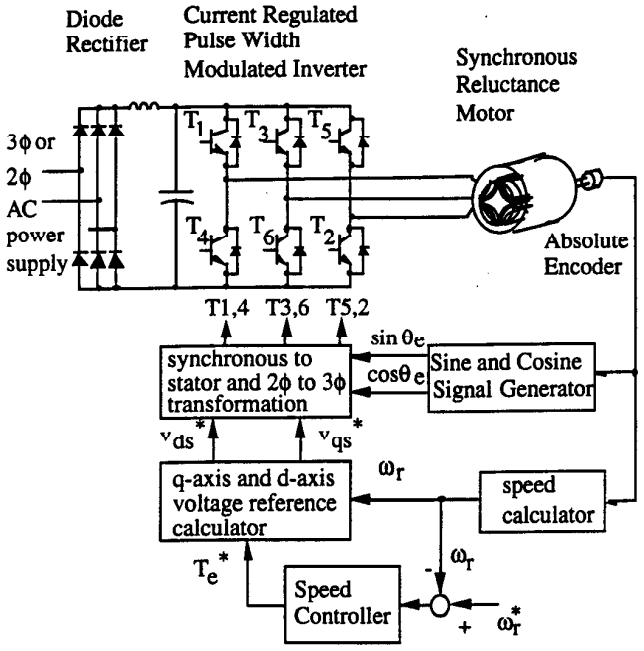

Fig. 4 General control configuration for a synchronous reluctance motor drive.

BLOCK DIAGRAM FOR IMPLEMENTING CURRENT SENSORLESS FIELD ORIENTED CONTROLLER

Figure 4 shows the overall control strategy proposed for controlling the torque and speed of a synchronous reluctance motor. By means of an absolute encoder or resolver, the sin and cosine of the angular position of the rotor is established. These sinusoidal components are used to refer those command stator voltages from the rotating (d-q) axes to the physical (stationary) reference frame. The encoder is also used to measure speed and, based on the speed measurement, the desired (command) values of v_{ds} and v_{qs} are established. The voltage command signals which are obtained in the synchronously rotating d-q frame are referred back to the stator frame before being used to switch the voltage source PWM inverted.

Figure 5 shows a control block diagram indicating the d-axis and q-axis voltage reference calculator for the current sensorless field oriented control. The voltage references in the d-q frame, v_{ds}^* and v_{qs}^*, are calculated in the q-axis and d-axis voltage reference calculator, which performs the calculations described by Eqs. 27, 28, 30 and 31 based on the motor parameters, the measured motor speed and the motor torque reference that is output from the speed controller. The details of the d-axis and q-axis voltage reference calculator are shown in Fig. 6(a) and (b). The two sets of the voltage references which are described by Eqs. 27, 28 and 30, 31 are to be switched between outputs of Fig. 6(a) and Fig. 6(b) according to the amplitude of the torque reference. The torque

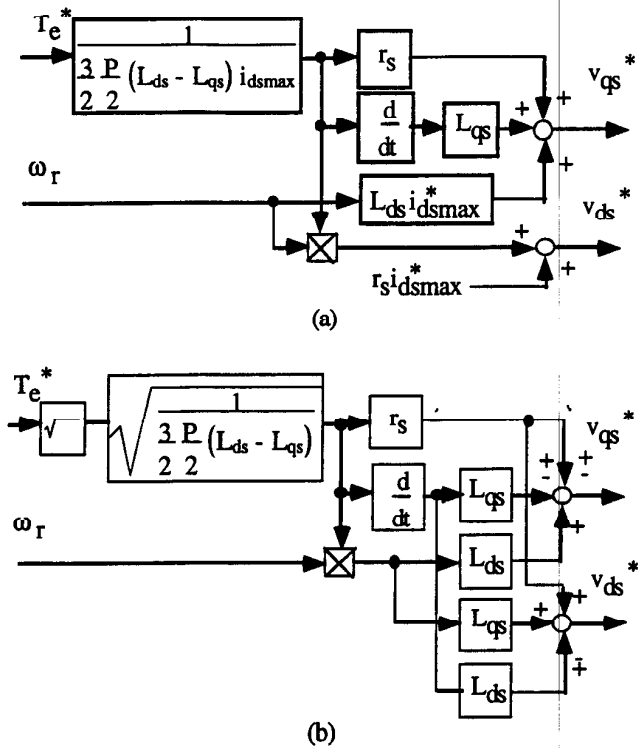

Fig. 6 Details of the d-axis and q-axis voltage reference calculator for the current sensorless field oriented control, (a) with the condition of $T_e^* > T_{e\text{-}idsmax}$ where d-axis current is constant at $i_{ds} = i_{dsmax}$ and (b) with the condition of $T_e^* < T_{e\text{-}idsmax}$ where $i_{ds} = i_{qs}$.

reference level which defines the switching point is given by Eq. 32.

The simplified voltage reference calculator can be realized by using only Fig. 6(a) by keeping d-axis current constant.

By utilizing the output of the position encoder, these voltage command signals are finally transformed from the synchronous to the stationary reference to form the actual switching commands of the inverted. The field weakening control can be achieved by changing the i_{dsmax}^* term in Fig. 6(a) according to the i_{dsmax}^* versus motor speed pattern shown in Fig. 7.

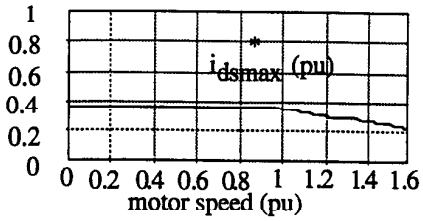

Fig. 7 Command current i_{dsmax}^* versus motor speed pattern for the field weakening of the current sensorless field oriented control.

EXPERIMENTAL RESULTS

A synchronous reluctance motor drive with the current sensorless field oriented control has been implemented in the laboratory in order to study the performance of the proposed control schemes. All the control functions are implemented with software and a conventional transistor inverted was used to drive the motor. The experimental synchronous reluctance motor used [5], has a saliency ratio L_{ds}/L_{qs} of 6.7 for unsaturated conditions and 6.4 for saturated conditions, and almost no cross coupling effects on both d- and q-axis magnetizing inductances.

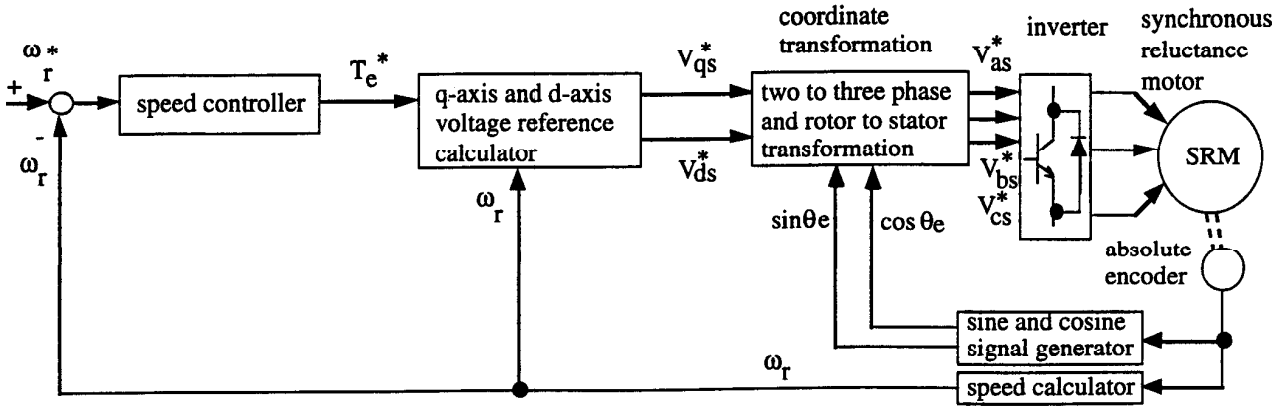

Fig. 5 Control block diagram of synchronous reluctance motor drive system showing the q-axis and d-axis voltage reference calculator.

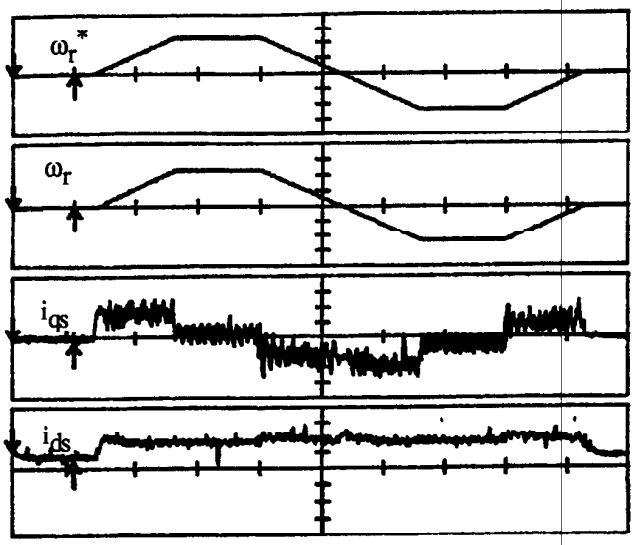

(a)

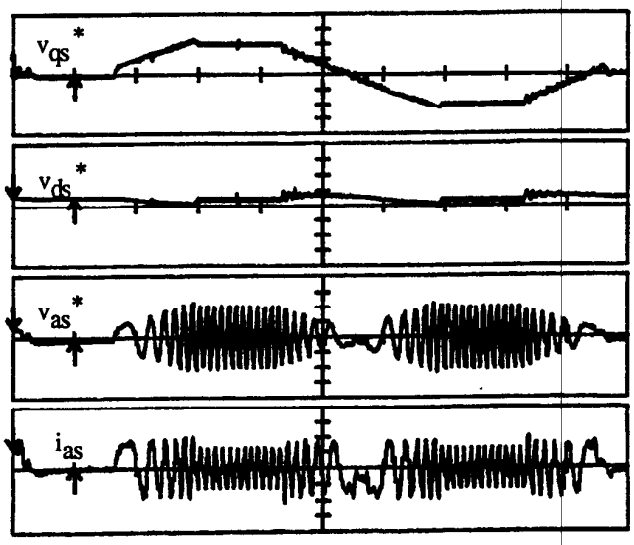

(b)

Fig. 8 Experimental results for the current sensorless field oriented control of the synchronous reluctance motor for four quadrant operation. The wave forms in (a) and (b) were recorded with the same conditions but at different timings. From top to bottom: (i) the speed reference (555 rpm/div.), (ii) the rotor shaft speed (555 rpm/div.), (iii) the monitored q-axis current i_{qs} (0.64 A/div.), (iv) the monitored d-axis current i_{ds} (0.64 A/div.), (v) the q-axis voltage reference v_{qs}^* (13.8V/div.), (vi) the d-axis voltage reference v_{ds}^* (13.8V/div.), (vii) the phase voltage reference v_{as}^* (13.8V/div.), (viii) the measure phase current i_{as} (1A/div.), the time scale is 0.2 sec./div.

Figure 8 shows one of the experimental results indicating that the synchronous reluctance motor is well controlled without current sensors over four quadrant operation, where the motor is accelerated from 0 rpm to top speed, 1300 rpm and decelerated to 0 rpm and then the speed is reversed up to -1300 rpm and decelerated to 0 rpm. The monitored d- and q-axis current wave forms show that the motor current vector is very well controlled without need for current sensors. The speed step response is shown in Fig. 9 where the speed control response is about 70 msec. It is demonstrated that the motor speed is nicely controlled and the control scheme is quite stable.

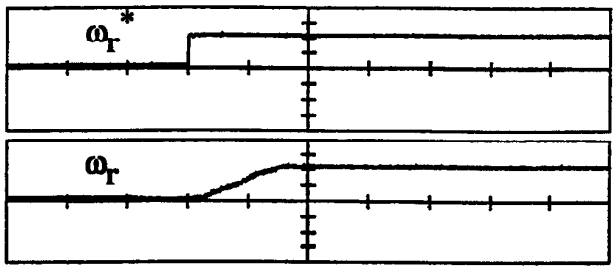

(a)

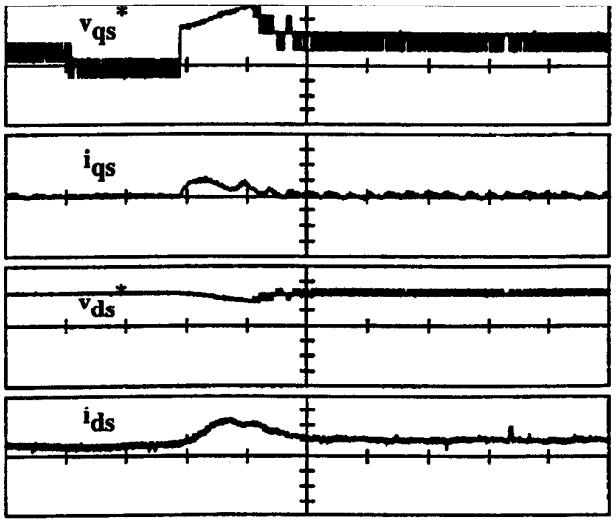

(b)

Fig. 9 Experimental results for the current sensorless field oriented control of the synchronous reluctance motor for speed step response, i.e., the speed command ω_r^* is changed from 43 rpm to 304 rpm. The wave forms in the figures (a) and (b) were recorded with same conditions but at different timings. From top to bottom: (i) the speed reference ω_r^* (139 rpm/div.), (ii) the rotor shaft speed ω_r (139 rpm/div.), (iii) the q-axis voltage reference v_{qs}^* (13.8V/div.), (iv) the monitored q-axis current i_{qs} (1.6 A/div.), (v) the d-axis voltage reference v_{ds}^* (13.8V/div.), (vi) the monitored d-axis current i_{ds} (0.64 A/div.), the time scale is 0.05 sec./div.

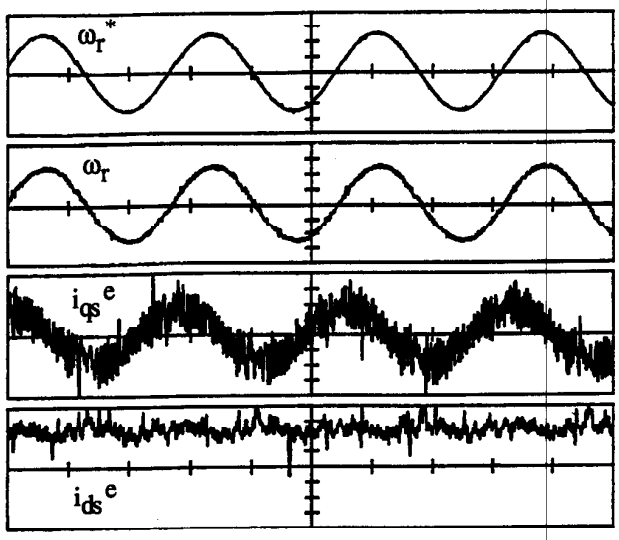

(a)

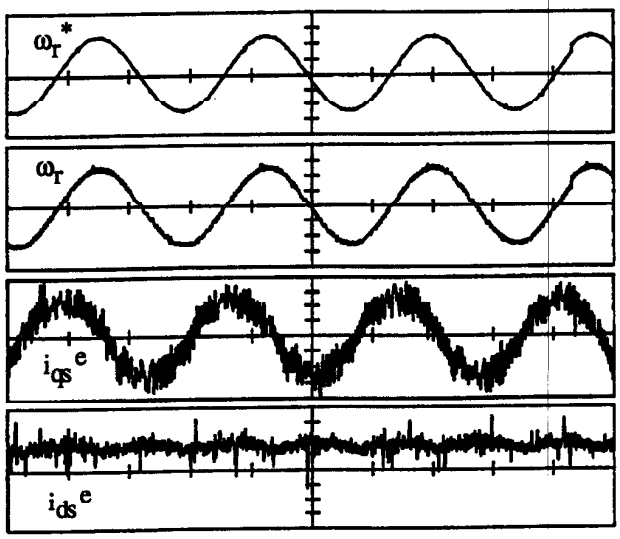

(b)

Fig. 10 Experimental comparison of two control schemes of synchronous reluctance motors for the sinusoidally varying speed reference. (a) the current sensorless field oriented control and (b) the field oriented control with current sensors. The speed command ω_r^* is changed sinusoidally from -348 rpm to 348 rpm. From top to bottom for both figures: (i) the speed reference ω_r^* (139 rpm/div.), (ii) the rotor shaft speed ω_r (139 rpm/div.), (iii) the monitored q-axis current i_{qs} (0.32 A/div.), (iv) the monitored d-axis current i_{ds} (0.32 A/div.), the time scale is 0.5 sec./div.

A comparison between two control schemes, corresponding to the current sensorless field oriented control scheme of this paper and a field oriented control with current sensors [4], is shown in Fig. 10. The wave forms clearly demonstrate that the current sensorless field oriented control scheme is competitive to the control scheme with current sensors.

CONCLUSION

In this work, control strategies, practical implementation and performance of a current sensorless field oriented control of synchronous reluctance motors have been presented. A field oriented control scheme without current sensors which includes the voltage reference calculator which generates the required voltage references from the torque command and the motor speed is proposed. Excellent control performance has been obtained, which indicates that the current sensorless field oriented control of synchronous reluctance motors can be applicable to practical high performance drive systems.

ACKNOWLEDGMENT

The authors are grateful to Gary E. Horst of Emerson Electric Co., St. Louis for the fabrication of the experimental synchronous reluctance motor

REFERENCES

1. T.A. Lipo, "Synchronous Reluctance Machines - A Viable Alternative for AC Drives?" SM100, Conference on the Evolution and Modern Aspects of Synchronous Machines, Aug. 1991, and Electric Machines and Power Systems, vol 19, pp. 659-671, Nov./Dec. 1991.
2. I. Boldea and S.A. Nasar,"Emerging Electric Machines with Axially Laminated Anisotropic Rotors: A Review, Electric Machines and Power Systems, vol. 19, Nov.Dec. 1991, pp. 673-703.
3. D. A. Staton, T. J. E. Miller and S. E. Wood, "Optimization of the Synchronous Reluctance Motor Geometry", Electrical Machines and Drives Conference Record, London, UK, 1991, pp. 156-160.
4. T. Matsuo and T. A. Lipo, "Field Oriented Control of Synchronous Reluctance Motor", Power Electronics Specialists Conference, June 1993, pp. 425-431.
5. T. Matsuo and T. A. Lipo, "Rotor Design Optimization of Synchronous Reluctance Motor", IEEE Power Engineering Summer Meeting, July 1993, to appear.
6. T. A. Lipo and T. Matsuo "Synchronous Reluctance Motors and Drives - A New Alternative. Section 1 - Performance of Synchronous Reluctance Motor Drive", Tutorial Notes, IEEE Annual Meeting. October 1992.